

ZWINT is a Promising Therapeutic Biomarker Associated with the Immune Microenvironment of Hepatocellular Carcinoma

Tong Lin ¹
Yingzhao Zhang¹
Zhimei Lin¹
Lisheng Peng ²

¹The Fourth Clinical Medical School, Guangzhou University of Chinese Medicine, Shenzhen, People's Republic of China; ²Department of Science and Education, Shenzhen Traditional Chinese Medicine Hospital, Shenzhen, People's Republic of China

Background: The prognosis of patients with advanced hepatocellular carcinoma (HCC) is still poor, effective therapeutic targets are needed. ZW10 interacting kinetochore protein (Zwint) is an essential component of the mitotic spindle checkpoint and is upregulated in cancers. Disappointing, the role of *ZWINT* in HCC has not been fully illuminated.

Methods: Multiple tools, including TIMER2.0, OncoPrint, GEPIA2, UALCAN, LinkedOmics, Kaplan–Meier Plotter, cBioPortal, and MethSurv, etc. were applied to comprehensively analyze the expression, genetic alternations, clinicopathological relevance, prognostic value, and DNA methylation of *ZWINT*, along with its correlations with immune infiltration in HCC. Besides, gene set enrichment analysis (GSEA) and protein–protein interaction (PPI) analysis were performed for the correlated genes of *ZWINT*, closely interconnected clusters and hub proteins in the PPI network were discovered to learn the underlying biological mechanisms.

Results: We found *ZWINT* was significantly upregulated in diverse cancers including HCC, compared with the corresponding normal controls. *ZWINT* upregulation was significantly associated with unfavorable clinicopathological features and survivals of HCC patients. Genetic alternations of *ZWINT* frequently occurred, which were linked to worse outcomes of HCC patients. The results of GSEA displayed *ZWINT* and its correlated genes might be components of condensed chromosomes and spindles, which participated in biological processes and signaling pathways involving DNA replication, cytokinesis, and cell cycle checkpoint, etc. Three highly interconnected clusters and 10 hub proteins were identified from the PPI network constructed with the correlated genes of *ZWINT*. Moreover, *ZWINT* expression was found positively correlated with infiltration levels of various immune cells, especially myeloid-derived suppressor cells.

Conclusion: This study demonstrated *ZWINT* might be a promising unfavorable prognostic biomarker and a therapeutic target of HCC, which could regulate HCC progression through cell division and immunosuppression.

Keywords: hepatocellular carcinoma, *ZWINT*, prognosis, immune infiltration, kinetochore

Introduction

Primary liver cancer is currently the sixth most prevalent and the third leading cause of cancer-related mortality in the world, up to 90% of which is hepatocellular carcinoma (HCC).¹ HCC is characterized by fast growth and early metastasis, most HCC patients are diagnosed at intermediate or advanced stages to miss curative treatments. Despite multitarget receptor tyrosine kinase inhibitors including Sorafenib and Lenvatinib improve the survival of advanced-stage HCC patients,

Correspondence: Lisheng Peng
Department of Science and Education,
Shenzhen Traditional Chinese Medicine
Hospital, No. 1 Fuhua Road, Futian
District, Shenzhen, Guangdong Province,
People's Republic of China
Email pls0556@gzucm.edu.cn

the benefits are unsatisfying and are frequently accompanied by side effects and treatment resistance.² Hence, there is always an urgent call for explorations of novel therapeutic candidates targeting the disease process.

Human ZW10 interacting kinetochore protein (Zwint1, encoded by *ZWINT*) is colocalized with Zeste White 10 (ZW10) at the kinetochore. Kinetochores are multiprotein complexes assembled onto microtubules linking chromosomes and spindles, thus mediate accurate chromosome segregation in mitosis.³ The spindle assembly checkpoint (SAC) is the main surveillance mechanism during chromosome segregation, and kinetochores are platforms for kinetochore-microtubule-attachment correction and SAC signaling.⁴ Zwint1 had been proved to be required for SAC during mitosis, whose inhibition would cause chromosome dysregulation and eventually induce cell apoptosis or tumorigenesis.^{5,6} Upregulation of *ZWINT* had been observed in various carcinomas and indicated poor outcomes of patients, including HCC,⁷ ovarian cancer,⁸ breast cancer,⁹ and glioblastoma.¹⁰ However, the role of *ZWINT* in HCC is still palely described.

In this work, we comprehensively analyzed the expression, genetic alternations, clinicopathologic and prognostic relevance, DNA methylation, and underlying functional mechanisms of *ZWINT* in HCC. Since interactions between cancer and the immune microenvironment largely influence cancer development and therapeutic responses,¹¹ the correlations between *ZWINT* and immune infiltration in HCC were also investigated. A study workflow is provided in [Supplementary Figure 1](#). This study will help to broaden the knowledge of *ZWINT* in HCC and may provide useful references for further studies and therapeutic strategies.

Materials and Methods

Analysis of Differential Expression of *ZWINT* Between Cancers and Adjacent Normal Tissues

The expression of *ZWINT* in various cancers and the corresponding normal tissues across all the Cancer Genome Atlas (TCGA) cancer types was analyzed using Tumor IMmune Estimation Resource Version 2.0 (TIMER2.0, <http://timer.cistrome.org>).¹² A metaanalysis of the differential mRNA expression of *ZWINT* in multiple cancers versus adjacent normal tissues was performed using OncoPrint (<https://www.oncoprint.org>), which is a web tool analyzing the published transcriptome data of over 18,000 cancer microarrays.¹³ The significance

thresholds in OncoPrint were set as: |fold change (FC)| > 2, *P* value < 0.001, and gene rank of top 10%.

Subsequently, the comparison of *ZWINT* expression between HCC and normal liver tissues was conducted by applying Gene Expression Profiling Interactive Analysis 2 (GEPIA2, <http://gepia2.cancer-pku.cn/>),¹⁴ using TCGA-liver hepatocellular carcinoma (LIHC) data (n = 369) and normal liver data (n = 369) from TCGA and GTEx datasets. The significance criteria were: |FC| > 2 and *P* value < 0.001.

Analysis of Associations Between *ZWINT* Expression and Clinicopathological Features of HCC Patients

UALCAN(<http://ualcan.path.uab.edu>)¹⁵ and LinkedOmics (<http://www.linkedomics.org>)¹⁶ are both online tools providing in-depth cancer omics analysis based on TCGA data. Associations between *ZWINT* expression and genders, ages, pathological stages, TNM stages, and tumor grades of HCC patients were explored using UALCAN and LinkedOmics.

Analysis of Prognostic Significance of *ZWINT* in HCC Patients

Associations between *ZWINT* expression and overall survival (OS), relapse-free survival (RFS), progression-free survival (PFS), and disease-free survival (DSS) of all HCC patients were evaluated using TCGA-LIHC data by Kaplan–Meier (KM) Plotter (<http://www.kmplot.com/>).¹⁷ The prognostic influence of *ZWINT* expression on OS and PFS of HCC patients with distinct clinicopathologic parameters was also evaluated. Here, all cases were divided into two groups by the median expression level of *ZWINT*.

Identification of Genetic Alternations of *ZWINT* in HCC

cBioPortal (<http://www.cbioportal.org>) is a web platform providing visual and multidimensional cancer genomics resources.^{18,19} Alternations of *ZWINT* including mutations, putative copy number alterations, and mRNA expression (z-scores relative to diploid samples with a score threshold of ± 2.0) were analyzed by cBioPortal using the data of 360 HCC samples from “TCGA, Firehose Legacy” dataset. Moreover, all cases were split into altered and unaltered groups, occurrence rates of vascular invasion and

survivals of HCC patients were compared between the two groups.

DNA Methylation Related Analysis for *ZWINT*

The comparison of global DNA methylation levels of *ZWINT* between HCC and normal liver tissues was performed using UALCAN. Correlations between *ZWINT* expression levels and its DNA methylation levels were analyzed using cBioPortal. Associations between methylation levels of cytosine-phosphate-guanine (CpG) sites of *ZWINT* and OS of HCC patients were evaluated using MethSurv (<https://biit.cs.ut.ee/methsurv/>).²⁰ Here, all cases were split into two groups by the median methylation level of a CpG site.

Gene Set Enrichment Analysis for Correlated Genes of *ZWINT*

Correlated genes of *ZWINT* were explored using TCGA-LIHC data ($n = 371$) by the LinkFinder module of LinkedOmics. Next, the correlated genes of *ZWINT* were sequenced to perform gene set enrichment analysis (GSEA) using Web-based Gene Set Analysis Toolkit (WebGestalt, <http://www.webgestalt.org/>).²¹ GSEA is an analytical method aiming to interpret genome-wide expression profiles by identifying whether an a priori defined set of genes shows statistically significant and concordant differences between two biological states.²² GSEA was conducted for gene ontology (GO) and Kyoto Encyclopedia of Genes and Genomes (KEGG) pathway categories. GO categories included biological process (BP), cellular component (CC), and molecular function (MF) terms. The category size was restricted between 5 and 2000, the number of permutations was limited below 500. A gene set satisfying $|\text{normalized enrichment score (NES)}| > 1$, adjusted P value < 0.05 , and false discovery rate (FDR) < 0.05 was considered significantly enriched.

Analysis of Protein–Protein Interaction of the Correlated Genes of *ZWINT*

The correlated genes of *ZWINT* meeting correlation coefficient (r) > 0.5 were included in protein–protein interaction (PPI) analysis using Search Tool for the Retrieval of Interacting Genes 11.0 (STRING 11.0, <https://string-db.org>). The settings were limited as follows: species of “homo sapiens”, interaction score > 0.7 , and FDR < 0.05 . Then, the PPI network was constructed using

Cytoscape software (version 3.7.0) with the disconnected nodes removed. Molecular Complex Detection (MCODE) plugin (version 1.6.1)²³ of Cytoscape was used to detect densely interacted clusters in the PPI network, with the cut-off parameters set as: node degree = 10, node score = 0.2, k-core = 2, and max depth = 100. Moreover, GO-BP functional annotation analysis was carried out for the clusters using Database for Annotation, Visualization, and Integrated Discovery (DAVID) server (<https://david.ncifcrf.gov/home.jsp>).²⁴

The top 10 hub proteins in the PPI network were identified using cytoHubba plugin²⁵ of Cytoscape depending on their degree values. Correlations between the hub genes and *ZWINT* in HCC were analyzed using TCGA-LIHC data by GEPIA2. The prognostic value of the hub genes in HCC patients was further discovered by KM Plotter, using the same grouping method as above.

Analysis of Correlations Between *ZWINT* Expression and Immune Infiltration in HCC

Correlations of *ZWINT* expression and the infiltration and some biomarkers' expression of diverse tumor-infiltrating immune cells (TIICs) in HCC were explored using TCGALIHC data integrating TIMER2.0 ($n = 371$) and TISIDB (<http://cis.hku.hk/TISIDB>) ($n = 371$).²⁶ The two portals both facilitate the investigation of tumor-immune interactions incorporating samples covering TCGA cancer types.

Statistical Analysis

Comparison of the mRNA expression or DNA methylation was performed using Wilcoxon test (TIMER2.0), Student's t -test (OncoPrint and UALCAN), one-way ANOVA test (GEPIA2), or Kruskal–Wallis test (LinkedOmics). KM curves and Log rank test were performed to identify the prognostic significance of a gene, global genetic alternation, or a methylated CpG site, and hazard ratio (HR), 95% confidence interval (CI), and P values were generated. The comparison of occurrence rates of vascular invasion between two groups was performed using Chi-squared test. Correlations between gene expression and its methylation level were performed using both Spearman and Pearson tests. Correlations between the expression of any two genes were evaluated using Pearson test. Spearman's method was applied to analyze correlations between gene expression and immune infiltration.

Correlation strength was measured by correlation coefficient (r) values: 0.00–0.19, 0.20–0.39, 0.40–0.59, 0.60–0.79, and 0.80–1.0 were very weak, weak, moderate, strong, and very strong, respectively.^{27,28} All tests were twotailed paired and P values < 0.05 were considered statistically significant. Besides, $FDR < 0.05$ was an additional criterion for functional enrichment analysis.

Results

Differential Expression of *ZWINT* in Cancers versus the Corresponding Normal Tissues

To begin with, differential expression of *ZWINT* between numerous cancers and the corresponding normal tissues was explored. *ZWINT* was found significantly highly expressed in 19 types of TCGA cancers; while lowly expressed in one kind of cancer in TIMER2.0 database, compared with adjacent normal tissues (Figure 1A). Similarly, in Oncomine, a total of 95 datasets suggested *ZWINT* was significantly up-expressed, whereas three datasets suggested it was down-expressed in cancers, compared with the corresponding normal controls (Figure 1B). Combining the findings from the two databases, *ZWINT* was significantly upregulated in diverse cancers, including bladder, breast, cervix, colon and rectum, esophagus, brain, head and neck, kidney, liver, lungs, and stomach, compared with the corresponding normal tissues.

Specifically, four datasets in Oncomine demonstrated *ZWINT* was significantly higher expressed in HCC than normal liver tissues, with the minimum FC of 3.391 (Figure 1C–F). Consistently, *ZWINT* was overexpressed in HCC compared with normal liver samples in GEPIA2 (Figure 1G).

Clinicopathological Relevance of *ZWINT* in HCC Patients

Already known that *ZWINT* was significantly highly expressed in HCC, its associations with clinicopathologic characteristics of HCC patients were investigated. The expression of *ZWINT* was significantly increased in almost all genders, ages, pathological stages, and tumor grades of HCC, compared with normal liver samples ($P < 0.05$) (Figure 2A–D). *ZWINT* expression was significantly elevated in HCC patients in Stage II–III, compared with that in Stage I ($P < 0.01$) (Figure 3C); and it was significantly correlated with pathological T stages of HCC patients ($P = 1.08E-03$) (Figure 2E). Nevertheless,

relationships between *ZWINT* expression and pathological N/M stages of patients could not be analyzed due to the insufficient sample size in the N1 and M1 groups (Supplementary Figure 2). Moreover, *ZWINT* expression was significantly higher in Grade-3 tumors than that in Grade-1/2 ones ($P < 0.01$) (Figure 3D). No significant difference was found for *ZWINT* expression in HCC patients of different genders and ages (Figure 2A and B). Briefly, increased *ZWINT* expression implied the advancement of pathological stages and histological grades of HCC patients.

Prognostic Value of *ZWINT* in HCC Patients

Next, associations between *ZWINT* expression and survivals of HCC patients were explored using KM Plotter. It was observed the high-expression of *ZWINT* was significantly related with worse OS (HR = 1.8, $P = 8.8E-04$), RFS (HR = 1.8, $P = 4.2E-04$), PFS (HR = 1.83, $P = 4.7E-05$), and DSS (HR = 2.07, $P = 1.3E-03$) of all HCC patients (Figure 2F).

The further analyses found *ZWINT* upregulation was significantly associated with unfavorable OS and PFS of male HCC patients, and patients with Grade-2 tumors, and patients without alcohol intake and a history of hepatitis. Additionally, high-expressed *ZWINT* suggested worse OS of HCC patients in pathological Stage II and Stage T2 according to the American Joint Committee on Cancer (AJCC) Staging Manual, also those with Grade-3 tumors (Table 1).

Genetic Alterations and DNA Methylation of *ZWINT* in HCC Patients

Genetic alterations of *ZWINT* in HCC patients were analyzed using cBioPortal. Overall, four kinds of alterations, including splice mutation, amplification and deep deletion of copy number alterations, and mRNA overexpression of *ZWINT* were observed in a total of 27 (7.74%) out of 360 HCC samples (Figure 3A), among which mRNA overexpression occurred the most frequently (6.59% of the included cases). Noteworthy, HCC patients with at least one kind of *ZWINT* alteration had a higher occurrence rate of vascular invasion (Figure 3B), and poorer OS (Figure 3C).

Then, we found *ZWINT* was similarly unmethylated in normal liver and HCC samples with beta values less than 0.05 (Figure 3D). DNA methylation levels of *ZWINT* were slightly negatively correlated with its expression levels in HCC (Spearman test: $r = -0.10$, $P = 0.0469$; Pearson test:

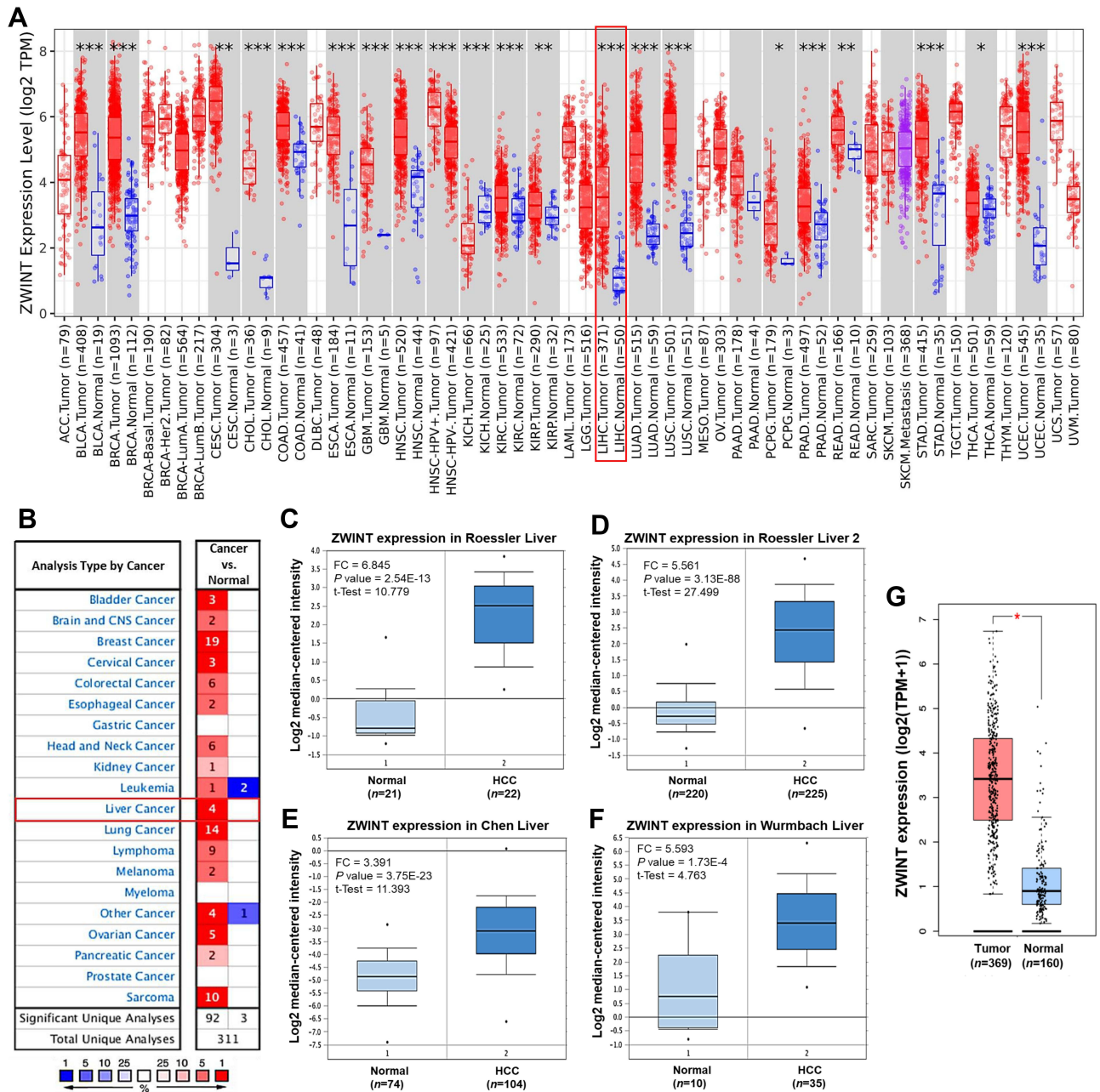


Figure I The differential expression of *ZWINT* between cancer and normal tissues. **(A)** Expression of *ZWINT* in tumors of diverse cancer types, compared with the corresponding normal tissues (TIMER2.0). Columns are in grey when normal data are available. * $P < 0.05$, ** $P < 0.01$, *** $P < 0.001$. **(B)** A summary of the datasets in which *ZWINT* were significantly up- (red) or down- (blue) expressed in various cancers, compared with the corresponding normal tissues (Oncomine). The cell color is paralleled with the best gene rank percentile for the analyses within the cell. Numbers in cells represent the counts of datasets. **(C–F)** Four datasets in which *ZWINT* was significantly upregulated in HCC, compared with normal liver samples (Oncomine). **(G)** *ZWINT* was markedly higher expressed in HCC than normal liver tissues in GEPIA2. * $|FC| > 2$ and $P < 0.001$.

Abbreviations: TPM, transcript per million; FC, fold change.

$r = -0.13$, $P = 0.0115$) (Figure 3E). Even though no significant difference was found in global methylation levels of *ZWINT* between HCC and normal liver tissues, we further investigated the prognostic significance its

methyated CpG sites in HCC patients. It turned out that the hypermethylation of one CpG site (cg16899823) of *ZWINT* significantly implied favorable OS of HCC patients (HR = 0.69, $P = 0.036$) (Figure 3F).

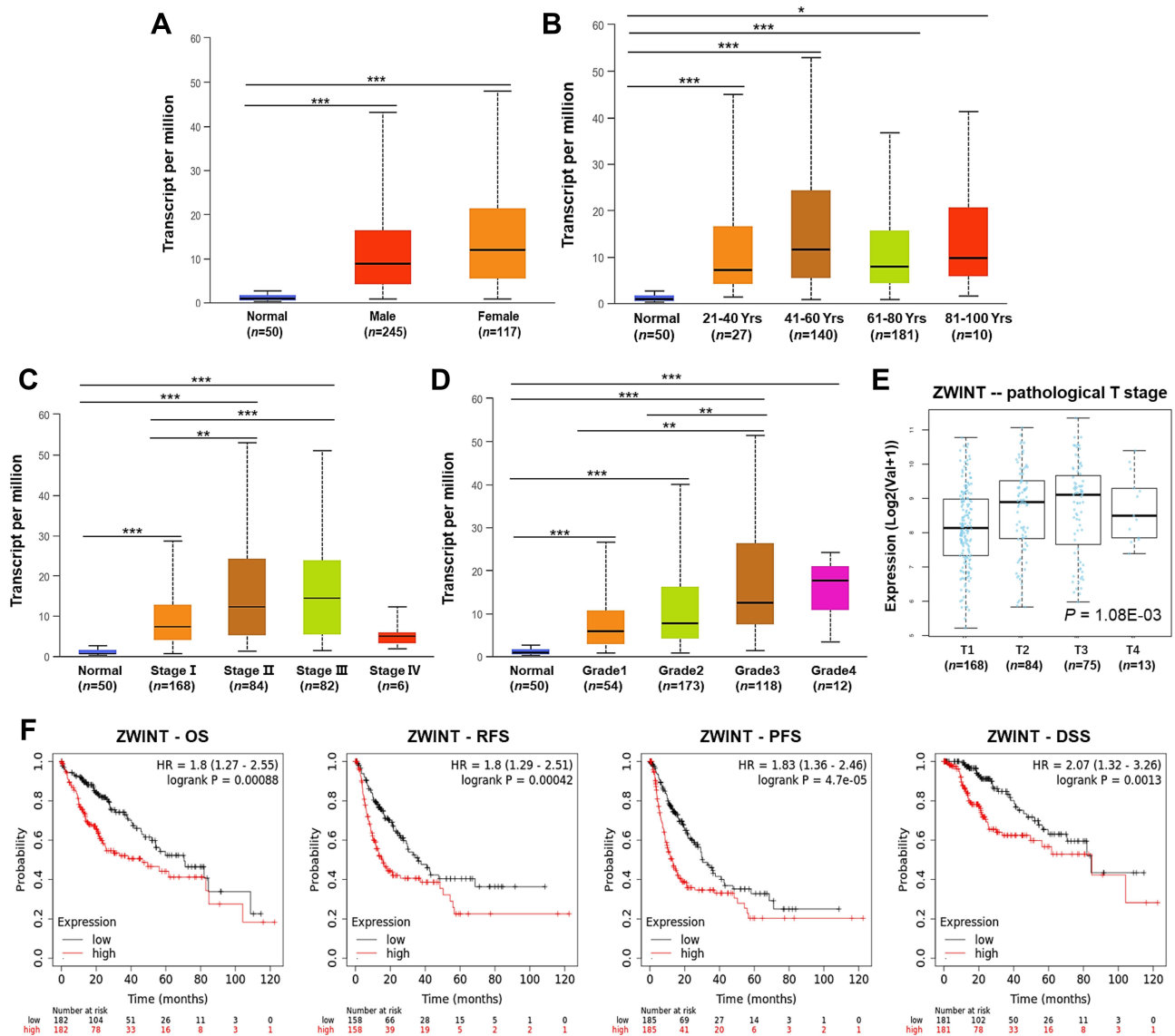


Figure 2 Clinicopathological and prognostic relevance of *ZWINT* in HCC patients. *ZWINT* expression in HCC patients with diverse (A) genders, (B) ages, (C) pathological stages, and (D) tumor grades (UALCAN). * $P < 0.05$, ** $P < 0.01$, *** $P < 0.001$. (E) The expression of *ZWINT* in HCC patients with different pathological T stages (LinkedOmics). (F) Survival curves present associations between *ZWINT* expression with OS, RFS, PFS, and DSS of HCC patients (KM Plotter). **Abbreviations:** OS, overall survival; RFS, relapse-free survival; PFS, progression-free survival; DSS, disease-specific survival; HR, hazard ratio; CI, confidence interval.

Potential Functions of the Correlated Genes of *ZWINT*

It turned out that 7519 genes were significantly positively and 4052 genes were negatively correlated with *ZWINT* expression (Figure 4A), the top 50 of which are shown in Figure 4B and C, respectively. The results of GSEA reflected the positively correlated genes of *ZWINT* mainly partook in the BPs of DNA replication, cytokinesis, and cell cycle checkpoint, etc.; while the negatively correlated genes were involved in acute inflammatory responses, peroxisome organization, fatty acid metabolic process, and endothelium

development, etc. (Figure 4D). The positively correlated genes composed condensed chromosomes, replication forks, spindles, heterochromatin, and microtubules; while the negatively correlated genes were components of protein-lipid complex, blood microparticle, and microbody, etc. (Figure 4E). As for the MF, the terms of single stranded DNA binding, damaged DNA binding, and motor activity, etc. were significantly enriched for the positively correlated genes, whereas the terms of the activity of oxidoreductase, monooxygenase, and electron transfer activity, etc., were enriched for the negatively correlated genes (Figure 4F).

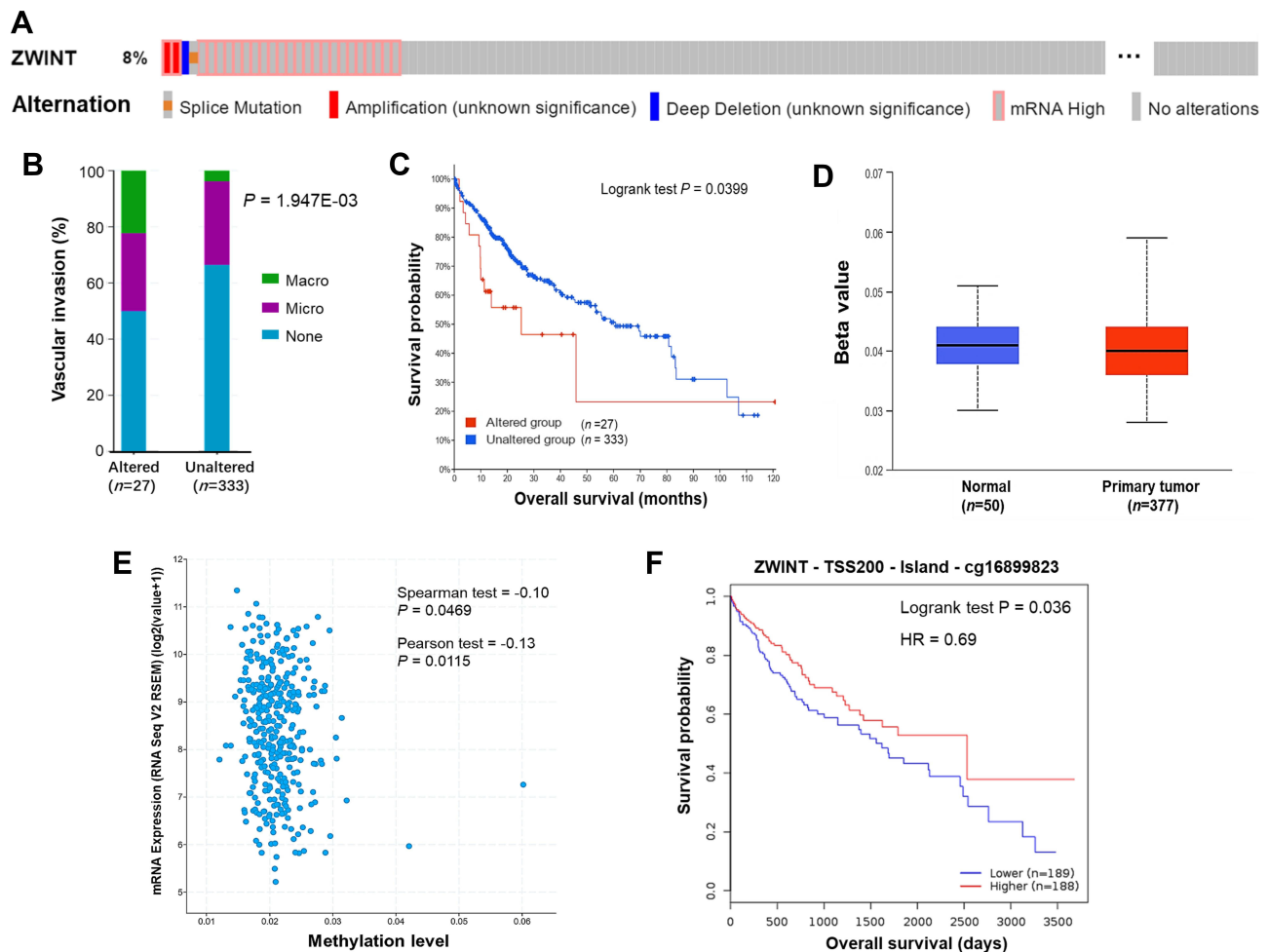


Figure 3 Genetic alterations and DNA methylation of *ZWINT* in HCC. **(A)** An overview of genetic alterations of *ZWINT* in HCC (cBioPortal). **(B)** The comparison of occurrence rates of vascular invasion between HCC patients with *ZWINT* altered or not. **(C)** The influence of the global alteration of *ZWINT* on the OS of HCC patients. **(D)** The promoter DNA methylation status of *ZWINT* in HCC and normal liver samples (UALCAN). **(E)** Correlations between DNA methylation levels and expression levels of *ZWINT* in HCC (cBioPortal). **(F)** A methylated CpG site of *ZWINT* was significantly associated with the OS of HCC patients (MethSurv).

Abbreviations: OS, overall survival; CpG, cytosinephosphate-guanine.

Moreover, the positively correlated genes of *ZWINT* were involved in signaling pathways of the cell cycle, DNA replication, and homologous recombination, etc., while the negatively correlated genes might regulate fatty acid degradation, steroid hormone biosynthesis, and primary bile acid biosynthesis, etc. (Figure 4G).

Highly Interconnected Clusters and the Hub Proteins in the PPI Network

The 250 positively and 9 negatively correlated genes of *ZWINT* meeting $r > 0.5$ were used to construct a PPI network. After abandoning the disconnected ones, the PPI network was composed of 189 proteins and 1879 interactions (Figure 5A). Cluster 1, Cluster 2, and Cluster

3 satisfying MCODE scores > 9 were identified using the MCODE plugin and were composed of 39, 10, and 24 proteins, respectively (Figure 5B). The functional annotation analysis indicated Cluster 1 genes mainly participated in sister chromatid cohesion, DNA replication, and telomere maintenance, etc.; Cluster 2 genes partook in G2/M transition of the mitotic cell cycle, spindle assembly, and cell division, etc.; Cluster 3 genes were involved in DNA replication, DNA repair, and DNA synthesis, etc. (Figure 5C–E).

Furthermore, cyclin-dependent kinase 1 (CDK1), minichromosome maintenance complex component (MCM) 3/4/5/7, kinesin family member 11 (KIF11), proliferating cell nuclear antigen (PCNA), breast cancer 1, early onset (BRCA1), exonuclease 1 (EXO1), and aurora kinase A (AURKA) were recognized as the

Table 1 Associations Between *ZWINT* Expression and OS and PFS of HCC Patients with Diverse Clinicopathological Parameters

| Clinicopathological parameters | n | OS | | n | PFS | |
|--------------------------------|-----|-----------------|-----------------|-----|-----------------|-----------------|
| | | HR (95% CI) | P | | HR (95% CI) | P |
| Gender | | | | | | |
| Male | 246 | 2.21(1.40–3.50) | 5.00E-04 | 249 | 2.01(1.39–2.89) | 1.00E-04 |
| Female | 118 | 1.41(0.81–2.46) | 0.22 | 121 | 1.55(0.93–2.58) | 0.09 |
| Pathological stage | | | | | | |
| I | 170 | 1.20(0.65–2.20) | 0.55 | 171 | 1.33(0.81–2.18) | 0.26 |
| II | 83 | 2.77(1.19–6.44) | 0.01 | 85 | 0.15 | 0.15 |
| III+IV | 87 | 1.48(0.82–2.67) | 0.19 | 90 | 1.44(0.85–2.46) | 0.17 |
| Tumor grade | | | | | | |
| 1 | 55 | 1.57(0.60–4.09) | 0.35 | 55 | 1.61(0.72–3.60) | 0.24 |
| 2 | 174 | 1.93(1.14–3.25) | 0.01 | 177 | 2.26(1.45–3.52) | 2.00E-04 |
| 3 | 118 | 1.96(1.06–3.65) | 0.03 | 119 | 1.60(0.97–2.64) | 0.06 |
| AJCC T stage | | | | | | |
| 1 | 180 | 1.40(0.78–2.50) | 0.26 | 181 | 1.39(0.86–2.25) | 0.18 |
| 2 | 90 | 2.53(1.18–5.47) | 0.01 | 93 | 1.53(0.88–2.65) | 0.13 |
| 3 | 78 | 1.66(0.90–3.05) | 0.10 | 80 | 1.29(0.74–2.28) | 0.37 |
| Alcohol consumption | | | | | | |
| Yes | 115 | 1.79(0.94–3.42) | 0.07 | 117 | 2.08(1.23–3.52) | 0.01 |
| No | 202 | 1.62(1.02–2.58) | 0.04 | 205 | 1.89(1.25–2.83) | 1.90E-03 |
| Hepatitis | | 0.73(0.22–2.43) | | | | |
| Yes | 150 | 1.22(0.64–2.32) | 0.55 | 153 | 1.46(0.92–2.32) | 0.11 |
| No | 167 | 2.33(1.46–3.71) | 2.00E-04 | 169 | 2.39(1.53–3.74) | 8.70E-05 |

Note: The results with statistical significance are in bold.

Abbreviations: OS, overall survival; PFS, progression-free survival; HR, hazard ratio; CI, confidence interval; AJCC, American Joint Committee on Cancer.

hub proteins in the PPI network based on their degree values (Figure 6A and Table 2). Among them, six and two different hub proteins belonged to Cluster 1 and Cluster 3 respectively. The gene expression of these hub proteins was all positively correlated with *ZWINT* with the minimum r value over 0.5, and the top one hub gene *CDK1* presented the closest correlation with *ZWINT* ($r = 0.87$, $P < 1E-04$) (Figure 6B–K). In addition, among the hub genes, the high expression of *CDK1*, *MCM5*, *KIF11*, *PCNA*, *MCM3*, *MCM7*, *BRCA1*, *EXO1*, and *AURKA* was significantly related to the unfavorable OS of HCC patients (Figure 6L).

Correlations Between *ZWINT* Expression and Immune Infiltration in HCC

Correlations between *ZWINT* expression and infiltration levels of diverse TIICs in HCC were investigated using TIMER2.0 server. As shown in Figure 7A, *ZWINT* expression was significantly positively correlated with the tumor purity ($r = 0.197$, $P = 2.31E-04$) and the infiltration level of myeloid dendritic cells (mDCs) ($r = 0.489$, $P = 3.77E-22$), CD4+ T cells ($r = 0.194$, $P = 2.83E-04$), regulatory T cells (Tregs) ($r = 0.285$, $P = 7.16E-08$), macrophages ($r = 0.3$, $P = 1.30E-08$), neutrophils ($r = 0.176$, $P = 1.05E-03$), B cells ($r = 0.377$, $P = 4.42E-13$), and myeloid-derived

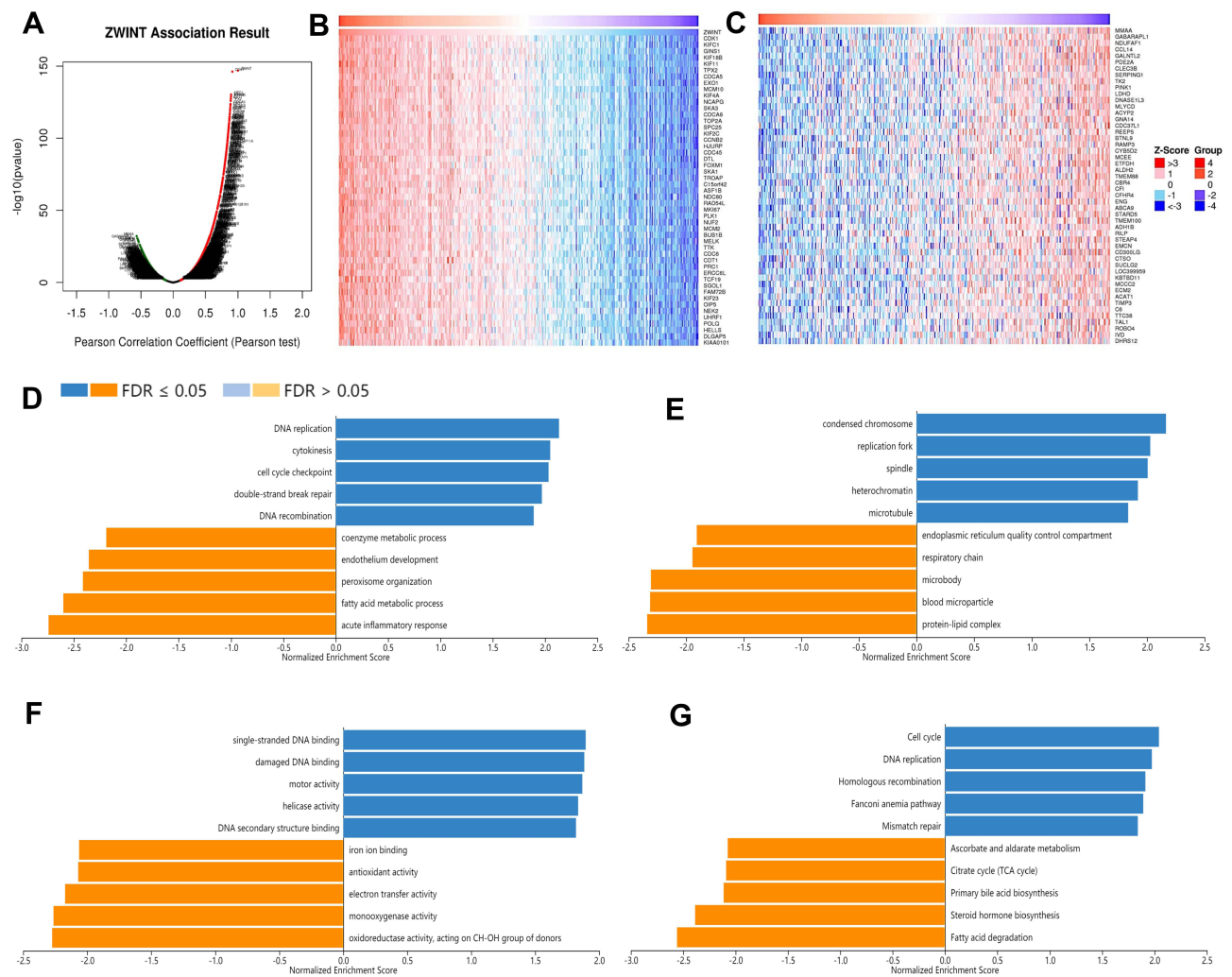


Figure 4 Correlated genes of *ZWINT* and the functional annotation based on GSEA. **(A)** Volcano plots show expressional correlations between *ZWINT* and its correlated genes in HCC (LinkedOmics). Red and green dots indicate positively and negatively correlated genes respectively. Heat maps showing the top 50 genes that were **(B)** positively and **(C)** negatively correlated with *ZWINT* in HCC (LinkedOmics). The top five significantly enriched **(D)** GO-BP, **(E)** GO-CC, **(F)** GO-MF, and **(G)** KEGG pathway terms for *ZWINT* correlated genes based on GSEA. Bars in blue or Orange represent positive or negative enrichment respectively. **Abbreviations:** GSEA, gene set enrichment analysis; GO, gene ontology; BP, biological process; CC, cellular component; MF, molecular function; KEGG, Kyoto Encyclopedia of Genes and Genome; FDR, false discovery rate.

suppressor cells (MDSCs) ($r = 0.707$, $P = 1.49E-53$). Whereas no significant correlation was observed between *ZWINT* expression and the infiltration of plasmacytoid CD8+ T cells, and natural killer (NK) cells.

Since distinct TIIC subtypes function differently, correlations between *ZWINT* expression and infiltration levels of some subsets of CD4+ T cells [helper T cells (Th) 1, 2, 17, and follicular helper T cells (Tfh)] were further analyzed using TISIDB. Correlations between the expression of *ZWINT* and biomarkers of tumor-associated macrophages (TAMs) were analyzed using TIMER2.0. We found the infiltration of Th1 cells ($r = -0.311$, $P = 9.65E-10$) was negatively, while that of Th2 cells ($r = 0.251$, $P = 9.85E-07$) was positively correlated with the

expression of *ZWINT*, both with a weak extent. However, no significant observation was found about Th17 and Tfh cells (Figure 7B). Moreover, *ZWINT* expression showed weakly positive correlations with the expression of biomarkers of TAMs, both M1- and M2-TAMs types ($P < 0.05$) (Figure 7C).

Discussion

During mitosis, sister chromatids of each chromosome must be accurately attached to the spindle microtubules to get equal segregation between two daughter cells. Defects in chromosome segregation give rise to chromosomal instability, which is a hallmark of cancers and genetic conditions. Proper kinetochore function is the key

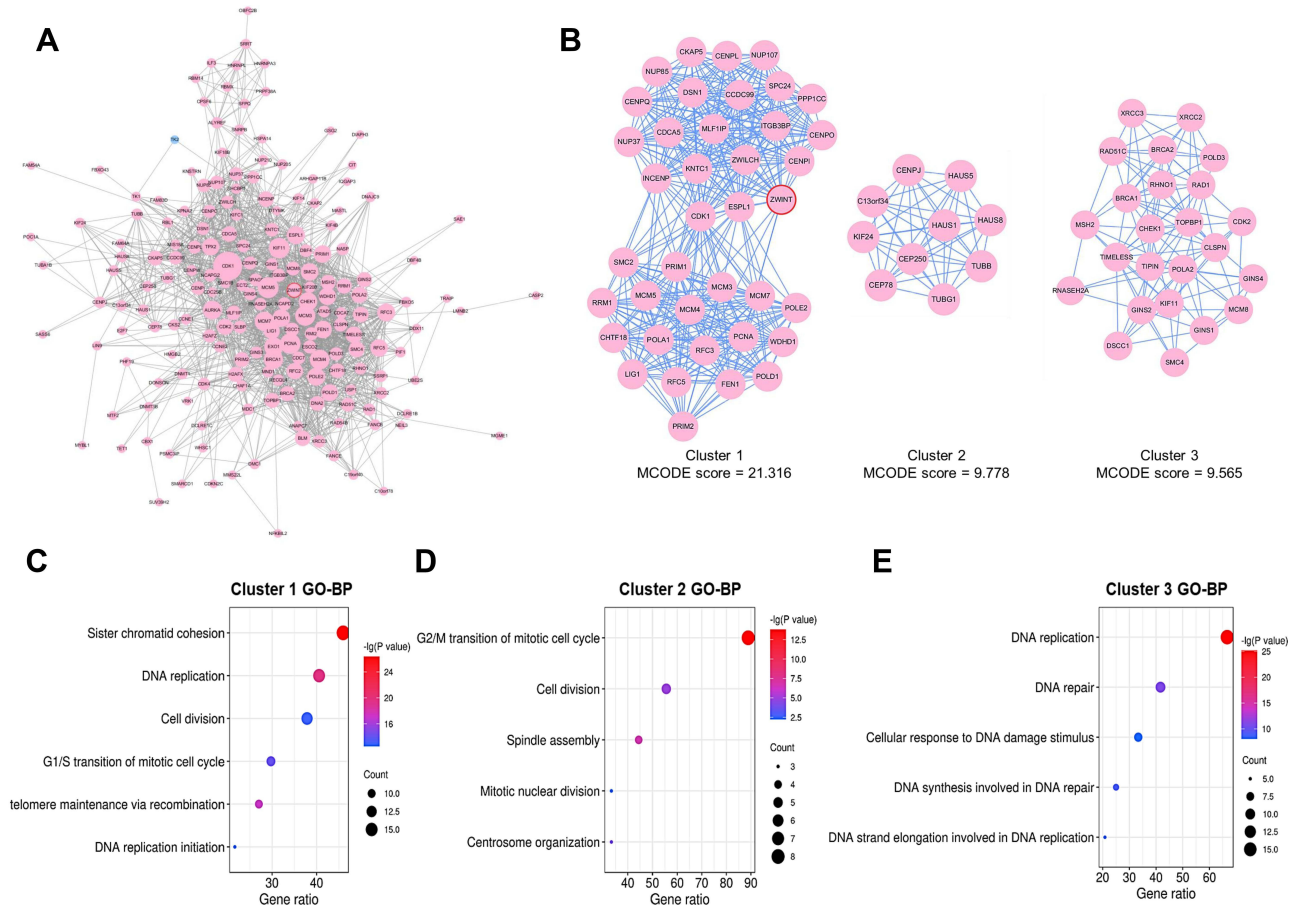


Figure 5 Highly interconnected clusters in the PPI network constructed by the correlated genes of *ZWINT*. **(A)** The PPI network constructed by the correlated genes of *ZWINT* meeting correlation coefficient > 0.5. Nodes in pink or blue represent positively or negatively correlated genes of *ZWINT* respectively, and node sizes signify degree values. Edges represent interactions among proteins, and edge thicknesses indicate interaction scores. **(B)** Three clusters with MCODE scores > 9 screened out from the PPI network. The top five GO-BP terms that were significantly enriched for the genes in **(C)** Cluster 1, **(D)** Cluster 2, and **(E)** Cluster 3, respectively.

to prevent aneuploidy. Deregulations of genes encoding kinetochore proteins are partially blamed for cancers, which therefore are considered promising anticancer strategies.^{29,30} In this work, comprehensive analyses were carried out to identify the potential prognostic and therapeutic values of a kinetochore protein, *ZWINT*, in HCC.

In previous studies, the mRNA and protein expression of *ZWINT* had been found significantly higher in HCC than noncancerous tissues, which indicated unfavorable clinical features (tumor size and number also recurrence tendency) and survival. Ectopic expression of *Zwint* would promote the proliferation of HCC cells.³¹ There were also bioinformatic studies implying *ZWINT* as a prognostic indicator of HCC, even an independent one.^{7,32} Consistently, we found *ZWINT* was significantly upregulated in various cancers including HCC, compared with the corresponding normal controls. We observed *ZWINT* overexpression significantly indicated the advancement of

pathological stages, histological grades, and worse survivals of HCC patients. And the adverse survival implications were significant even for those without alcohol intake nor hepatitis background. Furthermore, the overall genetic alternation of *ZWINT* was significantly linked with a higher incidence of vascular invasion and unfavorable OS of HCC patients. Despite this, no significant differential methylation between HCC and noncancer tissues was identified, suggesting DNA methylation might not be a major mechanism by which *ZWINT* regulated HCC development.

Functionally collaborative genes tend to show similar expressional profiles, whose proteins may constitute the same complex or regulate the same signaling. Therefore, GSEA for the co-expressed genes of *ZWINT* was performed to decipher its underlying functions. The positively correlated genes of *ZWINT* were generally components of condensed chromosomes, replication forks, and spindles,

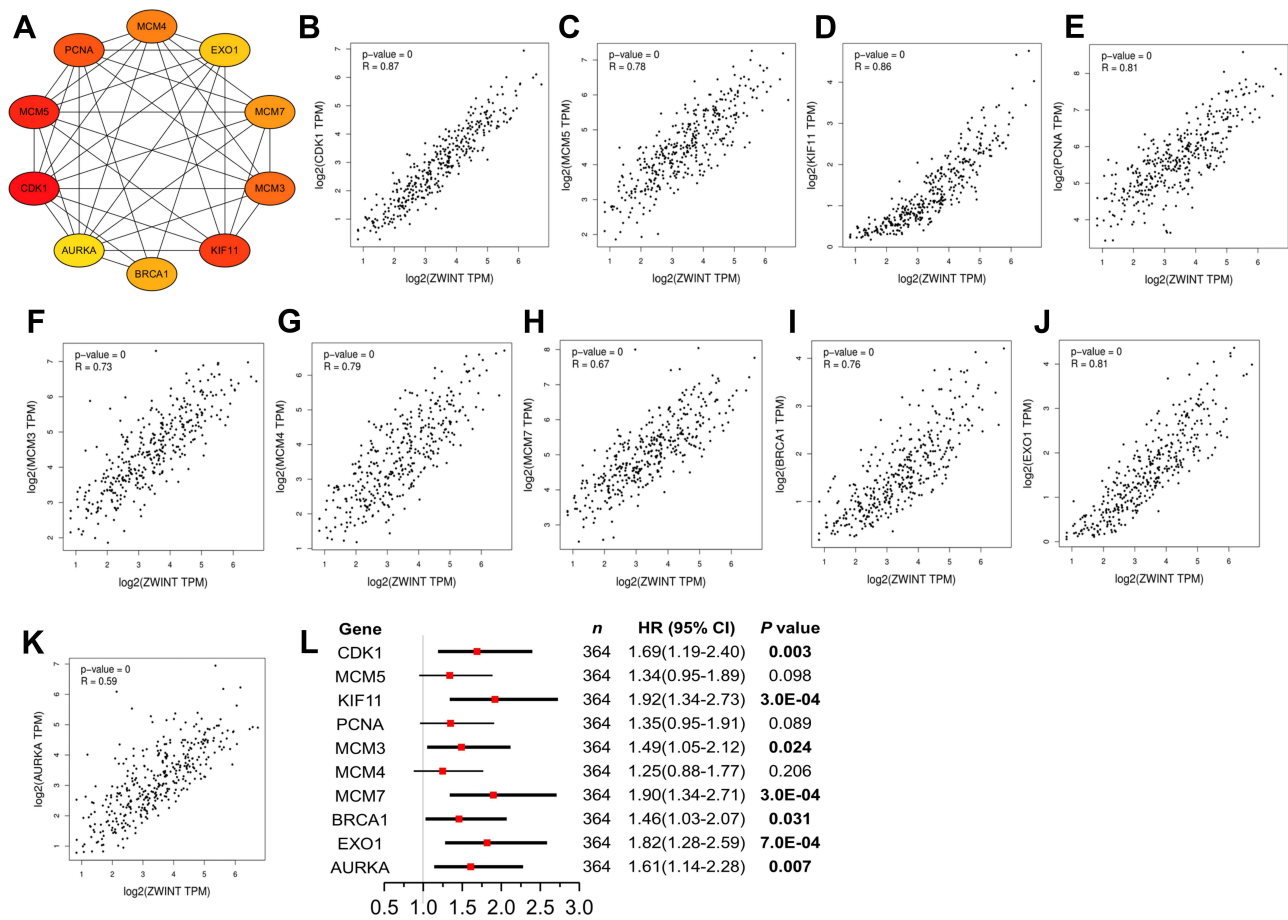


Figure 6 Analyses for the hub genes in the PPI network. **(A)** The top 10 hub genes in the PPI network. Redder colors indicate higher degree values. **(B–K)** Correlations between expression levels of *ZWINT* and **(B)** *CDK1*, **(C)** *MCM5*, **(D)** *KIF11*, **(E)** *PCNA*, **(F)** *MCM3*, **(G)** *MCM4*, **(H)** *MCM7*, **(I)** *BRCA1*, **(J)** *EXO1*, and **(K)** *AURKA* analyzed using Pearson test (GEPiA2). **(L)** Impacts of the hub genes on the OS of HCC patients. The results with statistical significance are in bold.

Abbreviation: OS, overall survival.

which participated in DNA replication, cytokinesis, and cell cycle control. While the negatively correlated genes of *ZWINT* might participate in inflammatory responses and fatty acid metabolism. At the protein level, closely interacting clusters in a PPI network might exert as molecular complexes or parts of signaling pathways. We found functions of the three clusters in the PPI network regarding DNA replication and repair were in line with the results of GSEA. Furthermore, *CDK1*, *MCM3/4/5/7*, *KIF11*, *PCNA*, *BRCA1*, *EXO1*, and *AURKA* were identified as the core contributors in the PPI network, and all of them were significantly associated with poor OS of HCC patients, except for *PCNA*. Notably, *CDK1* had a very strong correlation with *ZWINT*, which had also been described before.³¹

Chromosomal DNA replication in normal cells is strictly regulated by the replication licensing system to ensure it occurs only once per cell cycle. Dysregulation

of genes regulating DNA replication permits cells to escape from cell cycle inhibition and apoptosis, thereby confer a proliferative advantage, which is an outstanding feature of neoplastic cells.³³ CDKs are central regulators of the cell cycle including processes of

DNA replication, DNA repair, chromosome segregation, and mitotic exit.^{34,35} Cyclin B1/CDK1 regulates mitosis G2-M phase transition, during which CDK1 is controlled by checkpoint kinases to prevent aberrant DNA distributed to daughter cells.³⁴ MCM 2–7 proteins function as a helicase complex composing pre-replication complexes (pre-RCs), which license the initiation of DNA replication. Phosphorylation of CDKs can activate pre-RCs at the onset of DNA replication and inhibit pre-RCs reassembling to block rereplication.³⁶ CDKs interact with MCMs extensively. For instance, CDK-dependent MCM3 phosphorylation was indispensable for the formation of MCM2–7 complex;³⁷ and phosphorylation of

Table 2 The Hub Genes in the PPI Network

| Gene Symbol | Gene Name | Degree Value |
|-------------|--|--------------|
| CDK1 | Cyclin-dependent kinase 1 | 104 |
| MCM5 | Minichromosome maintenance complex component 5 | 64 |
| KIF11 | Kinesin family member 11 | 63 |
| PCNA | Proliferating cell nuclear antigen | 62 |
| MCM3 | Minichromosome maintenance complex component 3 | 60 |
| MCM4 | Minichromosome maintenance complex component 4 | 58 |
| MCM7 | Minichromosome maintenance complex component 7 | 56 |
| BRCA1 | Breast cancer 1, early onset | 55 |
| EXO1 | Exonuclease 1 | 54 |
| AURKA | Aurora kinase A | 53 |

MCM7 by Cyclin/Cdks in the M phase contributed to a proper mitotic exit.³⁸ High-expression of MCMs and CDKs had been recognized as early events during tumorigenesis, and they were considered promising diagnostic biomarkers for early detection and therapeutic targets of cancers.^{33,39}

KIFs participate in the organelle's transports, also chromosome and spindle movements during cell division, whose overexpression can induce genomic instability.

Upregulation of several KIFs, including *KIF11*, had been reported as biomarkers to predict unfavorable pathological characteristics and outcomes of HCC patients.^{40,41} PCNA is an auxiliary of DNA polymerases and forms DNA sliding clamps, which is essential for DNA replication and repair at the replication fork. Various cancer cells showed up to five to six-fold more *PCNA* expression than healthy cells, which likely contributed to high cell proliferation and might serve as a prognostic indicator for cancers.^{42,43} Despite this, *PCNA* was not associated with the survival of HCC patients in our study. *BRCA1* is a tumor-suppressive gene, especially for breast and ovarian cancer.

However, a recent bioinformatic study also indicated *BRCA1* played an evil role in HCC.⁴⁴ *EXO1* has 5' to 3' exonuclease and 5' structure-specific endonuclease activity, thus plays a pivotal role in DNA replication and repair, whose deletion can cause genomic instability and meiosis defects.⁴⁵ On the other side, *EXO1* overexpression promoted the proliferation and aggressiveness of HCC cells,⁴⁶ and was linked with advanced clinicopathological features

and poorer OS of HCC patients.⁴⁷ The activation of AURKA is necessary for chromosome segregation and mitotic progression in healthy cells. Meanwhile, upregulated AURKA could promote cell proliferation, epithelial-mesenchymal transition (EMT), and cancer stem cell self-renewal in multiple cancers. Recently, several AURKA inhibitors have been identified with anticancer activity in preclinical studies.⁴⁸ To sum up, the hub genes in the PPI network uniformly regulate the cell cycle, whose aberrance underlies malignant phenotypes of cancers, and most of them have been considered as cancer biomarkers.

CD8+ T cells and NK cells can be motivated by DCs and pro-inflammatory cytokines secreted by Th1 cells to exert effective immune surveillance to inhibit cancer.⁵⁰ In the current work, we found *ZWINT* expression significantly negatively correlated with the infiltration of Th1 cells, while positively correlated with the infiltration of DCs, macrophages, neutrophils, MDSCs, Th2 cells, Tregs, and B cells; and the biomarkers' expression of TAMs. But no observation was found for CD8+ T cells and NK cells. DCs, TAMs, tumor-associated neutrophils (TANs), and MDSCs are myeloid-derived cells leading to immune evasion and cancer progression.^{50,51} As professional antigen-presenting cells, DCs are equipped with immune stimulatory capacities once maturation; however, they often displayed tolerogenic phenotypes in cancers, influenced by the cytokines, enzymes, and growth factors from the tumor microenvironment (TME).^{52,53} TAMs and TANs can be polarized into anticancer M1/N1 subtypes or pro-cancer M2/N2 subtypes, depending on microenvironmental stimuli. M1-TAMs and N1-TANs can potentiate anticancer immunity, whereas M2-TAMs and N2-TANs can suppress adaptive immunity, promote angiogenesis and extracellular matrix remodeling to foster tumor progression. In general, the high density of TAMs and TANs may indicate invasive phenotypes, therapy resistance, and dismal outcomes of HCC patients.⁵⁴⁻⁵⁶ MDSCs are the main immunosuppressive cells in the TME with a capacity of blocking T-cell activation. Besides, they can increase Tregs' abundance, promote TAMs' M1-to-M2 transition and angiogenesis, etc., thereby promoting cancer.⁵⁷ Th1 cells express proinflammatory cytokines to activate immunity. In contrast, Th2, Th17, Tfh cells, and Tregs secrete inhibitory cytokines to foment immune escape. Therefore, an increased abundance of Th1 cells is generally associated with better treatment response and the survival of HCC patients,^{58,59} while Tregs did oppositely.⁶⁰ As for B cells, they seem to act dully in

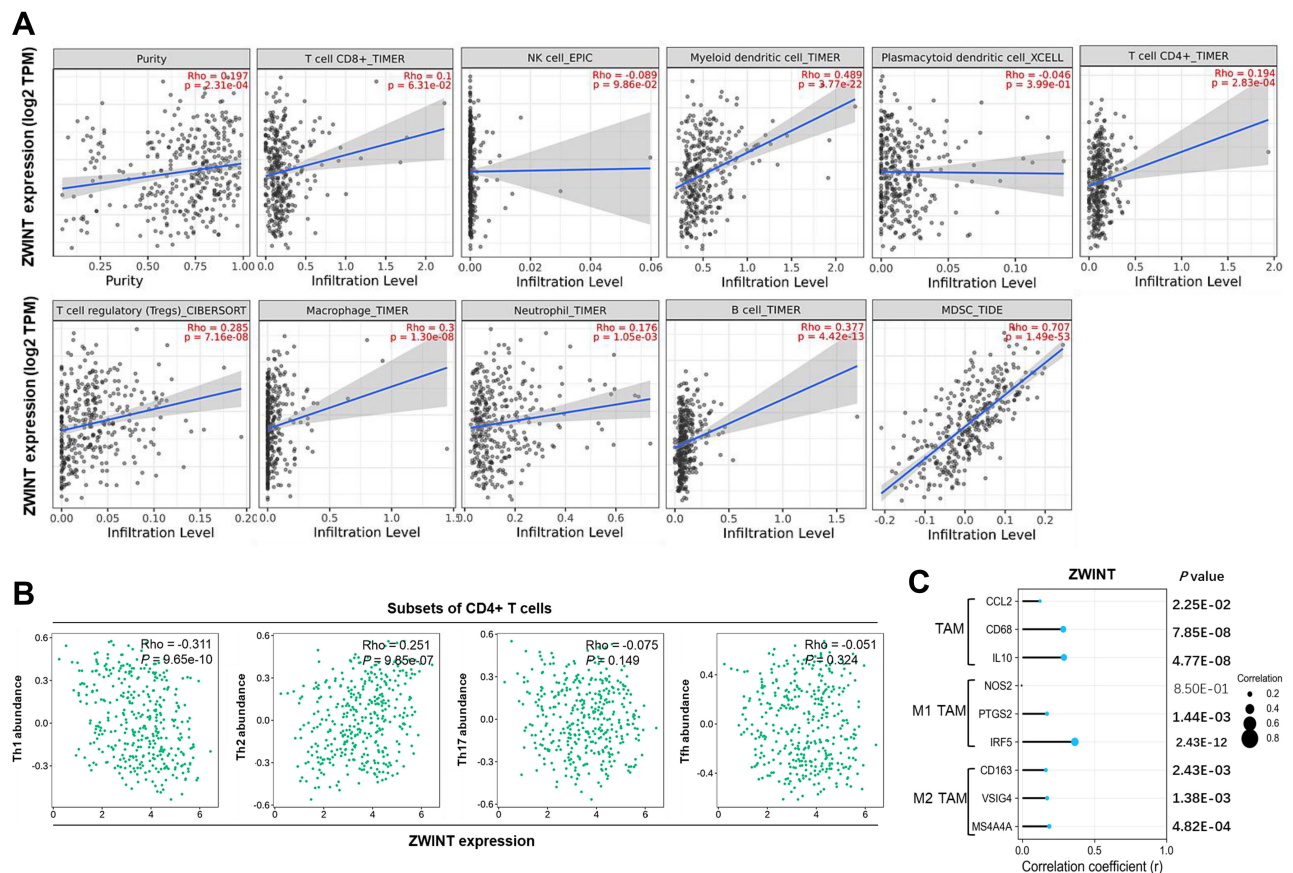


Figure 7 Correlations between *ZWINT* expression and immune infiltration in HCC. **(A)** Correlations between *ZWINT* expression and tumor purity, infiltration levels of CD8+ T cells, NK cells, mDCs, pDCs, CD4+ T cells, Tregs, macrophages, neutrophils, B cells, and MDSCs in HCC (TIMER2.0). **(B)** Correlations between *ZWINT* expression and infiltration levels of CD4+ T cell subsets in HCC (TISIDB). **(C)** Expressional correlations between *ZWINT* and biomarkers of TAM subsets. *P* values with statistical significance are in bold.

Abbreviations: NK cell, natural killer cell; mDC, myeloid dendritic cells; pDCs, plasmacytoid CD8, Treg, regulatory T cell; TAM, tumor-associated macrophage; MDSC, myeloid-derived suppressor cell; Th, helper T cell; Tfh, follicular helper T cell.

HCC depending on the secretion of inflammatory factors, and the consensus has not been reached.^{50,60,61} In short, *ZWINT* upregulation implied the rising infiltration of multiple immunosuppressive cells, which might partially explain its contributions to the HCC development.

Conclusions

This study depicted the role of *ZWINT* in HCC through comprehensive transcriptomic analyses. *ZWINT* is consistently up-expressed in multiple cancers, including HCC. The overexpression or alternations of *ZWINT* were significantly related to adverse clinicopathologic characteristics and survivals of HCC patients. *ZWINT* cooperated with its co-expressed genes to modulate DNA replication, DNA repair, and the cell cycle, whose variations underlay the uncontrolled proliferation of cancer cells. Apart from inducing chromosomal stability, we firstly reported *ZWINT* might promote HCC by raising the infiltration of various

immunosuppressive cells in the TME. Our study suggested *ZWINT* might be a universal unfavorable biomarker of cancers, which deserved more in-depth explorations and was prospected to be a novel therapeutic target regulating both cell division and immune microenvironment.

Data Sharing Statement

All data supporting the findings of this study had been provided in the article.

[Supplementary Materials](#), or were publicly available from the databases mentioned in the Materials and Methods section.

Ethics Approval and Consent to Participate

This study contained no data from human participants or animals performed by any of the authors, so the need

for ethical approval of it was waived by the Ethics Committee of Shenzhen Traditional Chinese Medicine Hospital.

Author Contributions

All authors contributed to conception, design, and data analysis; took part in drafting and revising the article; gave approval of the final version to be published; and agreed to be accountable for all aspects of the work.

Funding

There is no funding to report.

Disclosure

The authors declare no conflicts of interest in this work.

References

1. Ferlay J, Ervik M, Lam F, et al. Global cancer observatory: cancer today. Lyon, France: International Agency for Research on Cancer. Available from: <https://gco.iarc.fr/today>. Accessed March 25, 2021.
2. Duran SR, Jaquiss R. Hepatocellular carcinoma. *N Engl J Med*. 2019;381(1):e2. doi:10.1056/NEJMc1906565
3. Lin YT, Chen Y, Wu G, et al. Hec1 sequentially recruits Zwint-1 and ZW10 to kinetochores for faithful chromosome segregation and spindle checkpoint control. *Oncogene*. 2006;25(52):6901–6914. doi:10.1038/sj.onc.1209687
4. de Wolf B, Kops G. Kinetochores malfunction in human pathologies. *Adv Exp Med Biol*. 2017;1002:69–91. doi:10.1007/978-3-319-57127-0_4
5. Wang H, Hu X, Ding X, et al. Human Zwint-1 specifies localization of Zeste White 10 to kinetochores and is essential for mitotic checkpoint signaling. *J Biol Chem*. 2004;279(52):54590–54598. doi:10.1074/jbc.M407588200
6. Woo SD, Yeop YS, Chung WJ, et al. Zwint-1 is required for spindle assembly checkpoint function and kinetochore-microtubule attachment during oocyte meiosis. *Sci Rep*. 2015;5(15431). doi:10.1038/srep15431
7. Song X, Du R, Gui H, et al. Identification of potential hub genes related to the progression and prognosis of hepatocellular carcinoma through integrated bioinformatics analysis. *Oncol Rep*. 2020;43(1):133–146. doi:10.3892/or.2019.7400
8. Xu Z, Zhou Y, Cao Y, et al. Identification of candidate biomarkers and analysis of prognostic values in ovarian cancer by integrated bioinformatics analysis. *Med Oncol*. 2016;33(11):130. doi:10.1007/s12032016-0840-y
9. Li HN, Zheng WH, Du YY, et al. ZW10 interacting kinetochore protein may serve as a prognostic biomarker for human breast cancer: an integrated bioinformatics analysis. *Oncol Lett*. 2020;19(3):2163–2174. doi:10.3892/ol.2020.11353
10. Yang L, Han N, Zhang X, et al. Zwint: a potential therapeutic biomarker in patients with glioblastoma correlates with cell proliferation and invasion. *Oncol Rep*. 2020;43(6):1831–1844. doi:10.3892/or.2020.7573
11. Liang C. Chemokines and their receptors play important roles in the development of hepatocellular carcinoma. *World J Hepatol*. 2015;7(10):1390. doi:10.4254/wjh.v7.i10.1390
12. Li T, Fu J, Zeng S, et al. TIMER2.0 for analysis of tumor-infiltrating immune cells. *Nucleic Acids Res*. 2020;48(W1):W509–W514. doi:10.1093/nar/gkaa407
13. Rhodes DR, Kalyana-Sundaram S, Mahavisno V, et al. OncoPrint 3.0: genes, pathways, and networks in a collection of 18,000 cancer gene expression profiles. *Neoplasia*. 2007;9(2):166–180. doi:10.1593/neo.07112
14. Tang Z, Li C, Kang B, et al. GEPIA: a web server for cancer and normal gene expression profiling and interactive analyses. *Nucleic Acids Res*. 2017;45(W1):W98–W102. doi:10.1093/nar/gkx247
15. Chandrashekar DS, Bashel B, Balasubramanya S, et al. UALCAN: a portal for facilitating tumor subgroup gene expression and survival analyses. *Neoplasia*. 2017;19(8):649–658. doi:10.1016/j.neo.2017.05.002
16. Vasaikar SV, Straub P, Wang J, et al. LinkedOmics: analyzing multi-omics data within and across 32 cancer types. *Nucleic Acids Res*. 2018;46(D1):D956–D963. doi:10.1093/nar/gkx1090
17. Menyhart O, Nagy A, Györfy B. Determining consistent prognostic biomarkers of overall survival and vascular invasion in hepatocellular carcinoma. *R Soc Open Sci*. 2018;5(12):181006. doi:10.1098/rsos.181006
18. Cerami E, Gao J, Dogrusoz U, et al. The cBio cancer genomics portal: an open platform for exploring multidimensional cancer genomics data. *Cancer Discov*. 2012;2(5):401–404. doi:10.1158/2159-8290.CD12-0095
19. Gao J, Aksoy BA, Dogrusoz U, et al. Integrative analysis of complex cancer genomics and clinical profiles using the cBioportal. *Sci Signal*. 2013;6(269):11. doi:10.1126/scisignal.2004088
20. Modhukur V, Iljasenko T, Metsalu T, et al. MethSurv: a web tool to perform multivariable survival analysis using DNA methylation data. *Epigenomics-Uk*. 2018;10(3):277–288. doi:10.2217/epi-2017-0118
21. Liao Y, Wang J, Jaehnig EJ, et al. WebGestalt 2019: gene set analysis toolkit with revamped UIs and APIs. *Nucleic Acids Res*. 2019;47(W1):W199–W205. doi:10.1093/nar/gkz401
22. Subramanian A, Tamayo P, Mootha VK, et al. Gene set enrichment analysis: a knowledge-based approach for interpreting genome-wide expression profiles. *Proc Natl Acad Sci U S A*. 2005;102(43):15545–15550. doi:10.1073/pnas.0506580102
23. Bader GD, Hogue CW. An automated method for finding molecular complexes in large protein interaction networks. *BMC Bioinform*. 2003;4(2). doi:10.1186/1471-2105-4-2
24. Huang DW, Sherman BT, Lempicki RA. Systematic and integrative analysis of large gene lists using DAVID bioinformatics resources. *Nat Protoc*. 2009;4(1):44–57. doi:10.1038/nprot.2008.211
25. Chin CH, Chen SH, Wu HH, et al. CytoHubba: identifying hub objects and sub-networks from complex interactome. *BMC Syst Biol*. 2014;8 Suppl 4(Suppl 4):S11. doi:10.1186/1752-0509-8-S4-S11
26. Ru B, Wong CN, Tong Y, et al. TISIDB: an integrated repository portal for tumor-immune system interactions. *Bioinformatics*. 2019;35(20):4200–4202. doi:10.1093/bioinformatics/btz210
27. Pan J, Zhou H, Cooper L, et al. LAYN is a prognostic biomarker and correlated with immune infiltrates in gastric and colon cancers. *Front Immunol*. 2019;10(6). doi:10.3389/fimmu.2019.00006
28. Xiao Z, Hu L, Yang L, et al. TGFβ2 is a prognostic-related biomarker and correlated with immune infiltrates in gastric cancer. *J Cell Mol Med*. 2020;24(13):7151–7162. doi:10.1111/jcmm.15164
29. Ovejero S, Bueno A, Sacristán MP. Working on genomic stability: from the s-phase to mitosis. *Genes*. 2020;11(2):225. doi:10.3390/genes11020225
30. Benzi G, Piatti S. Killing two birds with one stone: how budding yeast MPS1 controls chromosome segregation and spindle assembly checkpoint through phosphorylation of a single kinetochore protein. *Curr Genet*. 2020;66(6):1037–1044. doi:10.1007/s00294-020-01091-x
31. Ying H, Xu Z, Chen M, et al. Overexpression of Zwint predicts poor prognosis and promotes the proliferation of hepatocellular carcinoma by regulating cell-cycle-related proteins. *Oncotargets Ther*. 2018;11:689–702. doi:10.2147/OTT.S152138

32. Zhu W, Zhang Q, Liu M, et al. Identification of DNA repair-related genes predicting pathogenesis and prognosis for liver cancer. *Cancer Cell Int.* 2021;21(1):81. doi:10.1186/s12935-021-01779-1
33. Enders GH, Maude SL. Traffic safety for the cell: influence of cyclin-dependent kinase activity on genomic stability. *Gene.* 2006; 371(1):1–6. doi:10.1016/j.gene.2005.11.017
34. Lukasik P, Załuski M, Gutowska I. Cyclin-dependent kinases (CDK) and their role in diseases development-review. *Int J Mol Sci.* 2021;22(6):2935. doi:10.3390/ijms22062935
35. Palmer N, Kaldis P. Less-well known functions of cyclin/CDK complexes. *Semin Cell Dev Biol.* 2020;107:54–62. doi:10.1016/j.semedb.2020.04.003
36. Araki H. Cyclin-dependent kinase-dependent initiation of chromosomal DNA replication. *Curr Opin Cell Biol.* 2010;22(6):766–771. doi:10.1016/j.ceb.2010.07.015
37. Lin DI, Aggarwal P, Diehl JA. Phosphorylation of MCM3 on Ser-112 regulates its incorporation into the MCM2–7 complex. *Proc Natl Acad Sci U S A.* 2008;105(23):8079–8084. doi:10.1073/pnas.0800077105
38. Wei Q, Li J, Liu T, et al. Phosphorylation of minichromosome maintenance protein 7 (MCM7) by cyclin/cyclin-dependent kinase affects its function in cell cycle regulation. *J Biol Chem.* 2013;288(27):19715–19725. doi:10.1074/jbc.M112.449652
39. Mughal MJ, Mahadevappa R, Kwok HF. DNA replication licensing proteins: saints and sinners in cancer. *Semin Cancer Biol.* 2019;58:11–21. doi:10.1016/j.semcancer.2018.11.009
40. Li X, Huang W, Huang W, et al. Kinesin family members KIF2C/4A/10/11/14/18B/20A/23 predict poor prognosis and promote cell proliferation in hepatocellular carcinoma. *Am J Transl Res.* 2020;12(5):1614–1639.
41. Hu ZD, Jiang Y, Sun HM, et al. KIF11 promotes proliferation of hepatocellular carcinoma among patients with liver cancers. *Biomed Res Int.* 2021;2021:2676745. doi:10.1155/2021/2676745
42. Horsfall AJ, Abell AD, Bruning JB. Targeting PCNA with peptide mimetics for therapeutic purposes. *Chembiochem.* 2020;21(4):442–450. doi:10.1002/cbic.201900275
43. Lv Q, Zhang J, Yi Y, et al. Proliferating cell nuclear antigen has an association with prognosis and risks factors of cancer patients: a systematic review. *Mol Neurobiol.* 2016;53(9):6209–6217. doi:10.1007/s12035-015-9525-3
44. Mei J, Wang R, Xia D, et al. Brcal is a novel prognostic indicator and associates with immune cell infiltration in hepatocellular carcinoma. *DNA Cell Biol.* 2020;39(10):1838–1849. doi:10.1089/dna.2020.5644
45. Keijzers G, Bakula D, Petr MA, et al. Human exonuclease 1 (EXO1) regulatory functions in DNA replication with putative roles in cancer. *Int J Mol Sci.* 2018;20(1). doi:10.3390/ijms20010074
46. Yang G, Dong K, Zhang Z, et al. EXO1 plays a carcinogenic role in hepatocellular carcinoma and is related to the regulation of FOXP3. *J Cancer.* 2020;11(16):4917–4932. doi:10.7150/jca.40673
47. Dai Y, Tang Z, Yang Z, et al. EXO1 overexpression is associated with poor prognosis of hepatocellular carcinoma patients. *Cell Cycle.* 2018;17(19–20):2386–2397. doi:10.1080/15384101.2018.1534511
48. Du R, Huang C, Liu K, et al. Targeting AURKA in cancer: molecular mechanisms and opportunities for cancer therapy. *Mol Cancer.* 2021;20(1):15. doi:10.1186/s12943-020-01305-3
49. Endig J, Buitrago-Molina LE, Marhenke S, et al. Dual role of the adaptive immune system in liver injury and hepatocellular carcinoma development. *Cancer Cell.* 2016;30(2):308–323. doi:10.1016/j.ccell.2016.06.009
50. Lu C, Rong D, Zhang B, et al. Current perspectives on the immunosuppressive tumor microenvironment in hepatocellular carcinoma: challenges and opportunities. *Mol Cancer.* 2019;18(1). doi:10.1186/s12943019-1047-6
51. Chaib M, Chauhan SC, Makowski L. Friend or foe? Recent strategies to target myeloid cells in cancer. *Front Cell Dev Biol.* 2020;8:(351). doi:10.3389/fcell.2020.00351
52. Sittig SP, de Vries I, Schreibelt G. Primary human blood dendritic cells for cancer immunotherapy tailoring the immune response by dendritic cell maturation. *Biomedicines.* 2015;3(4):282–303. doi:10.3390/biomedicines3040282
53. Volovitz I, Melzer S, Amar S, et al. Dendritic cells in the context of human tumors: biology and experimental tools. *Int Rev Immunol.* 2016;35(2):116–135. doi:10.3109/08830185.2015.1096935
54. Masucci MT, Minopoli M, Carriero MV. Tumor associated neutrophils. Their role in tumorigenesis, metastasis, prognosis and therapy. *Front Oncol.* 2019;9:1146. doi:10.3389/fonc.2019.01146
55. Piccard H, Muschel RJ, Opdenakker G. On the dual roles and polarized phenotypes of neutrophils in tumor development and progression. *Crit Rev Oncol Hematol.* 2012;82(3):296–309. doi:10.1016/j.critrevonc.2011.06.004
56. Keeley T, Costanzo-Garvey DL, Cook LM. Unmasking the many faces of tumor-associated neutrophils and macrophages: considerations for targeting innate immune cells in cancer. *Trends Cancer.* 2019;5(12):789–798. doi:10.1016/j.trecan.2019.10.013
57. Schupp J, Krebs FK, Zimmer N, et al. Targeting myeloid cells in the tumor sustaining microenvironment. *Cell Immunol.* 2019;343:103713. doi:10.1016/j.cellimm.2017.10.013
58. Yang Y, Kim S, Seki E. Inflammation and liver cancer: molecular mechanisms and therapeutic targets. *Semin Liver Dis.* 2019;39(01):26–42. doi:10.1055/s-0038-1676806
59. Richardson JR, Schöllhorn A, Gouttefangeas C, et al. CD4+ T cells: multitasking cells in the duty of cancer immunotherapy. *Cancers.* 2021;13(4):596. doi:10.3390/cancers13040596
60. Ringelhan M, Pfister D, Connor O, et al. The immunology of hepatocellular carcinoma. *Nat Immunol.* 2018;19(3):222–232. doi:10.1038/s41590-018-0044-z
61. Garnelo M, Tan A, Her Z, et al. Interaction between tumour-infiltrating b cells and t cells controls the progression of hepatocellular carcinoma. *Gut.* 2017;66(2):342–351. doi:10.1136/gutjnl-2015-310814